THE JOURNAL OF PHYSICAL CHEMISTRY B

ARTICLE

pubs.acs.org/JPCB

Density of States and Wave Function Localization in Disordered Conjugated Polymers: A Large Scale Computational Study

Nenad Vukmirović*[,†,‡] and Lin-Wang Wang[†]

[†]Materials Sciences Division, Lawrence Berkeley National Laboratory, Berkeley, California 94720, United States

[‡]Scientific Computing Laboratory, Institute of Physics Belgrade, University of Belgrade, Pregrevica 118, 11080 Belgrade, Serbia

Supporting Information

ABSTRACT: We present large-scale calculations of electronic structure of strongly disordered conjugated polymers. The calculations have been performed using the density functional theory based charge patching method for the construction of single-particle Hamiltonian and the overlapping fragments method for the efficient diagonalization of that Hamiltonian. We find that the hole states are localized due to the fluctuations of the electrostatic potential and not by the breaks in the conjugation of the polymer chain. The tail of the density of hole states exhibits an exponentially decaying behavior. The main features of the electronic structure of the system can be described by an one-dimensional nearest neighbor tight-binding model with a correlated Gaussian distribution of on-site energies and constant off-site coupling elements.

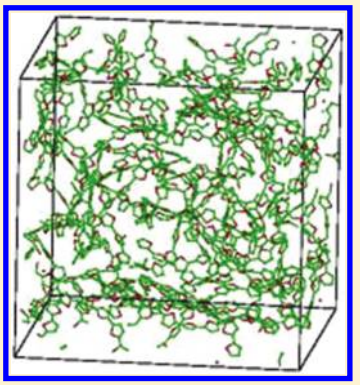

INTRODUCTION

The density of electronic states and the wave function localization lengths are the key quantities that determine the electronic transport in conjugated polymers, the topic of high current interest for application in organic electronic devices.[1−4] Despite that, there is still a lack of understanding of the factors that determine them and the lack of tools for their measurement or prediction.

The density of electronic states is often extracted from fits of a transport model to the experimental measurements of the temperature dependence of the mobility.[5−8] A transport model however assumes already a certain functional form of the density of states, the spatial distribution of electronic states, and the transition rates between the states.[5−10] The parameters of these functional forms are then adjusted to reproduce the experimental mobility measurements. With several such assumptions at hand, there is a concern whether the density of states obtained from such a fit is really the physical density of states. If any of the underlying assumptions is incorrect, then one can still obtain some effective density of states that, in combination with the rest of the model, fits the experiment. Our recent study[11] has, for example, shown that the Miller−Abrahams form of the transition rates between the states can yield quite inaccurate results. Furthermore, there is no consensus in the literature about the functional form of the electronic density of states. The most widely used ones are the tail of the Gaussian[5,7−10] or the tail of the exponential distribution.[6,10] Experimental techniques that more directly probe the density of electronic states based on Kelvin probe force microscopy[12] or the measurements on the electrochemically gated transistor[13] are starting to appear but are not yet widely practiced.

The understanding of the localization properties of the electronic states is also far from complete. On the experimental side, probing of the wave functions of individual states in disordered systems is quite a challenge. The main question that one should address related to the localization properties is whether the electronic states near the band edge are well-localized and become more extended as one goes away from the band edge with a possible mobility edge or if the situation is opposite. There are arguments that could support both of these scenarios. A widely used picture of wave function localization in conjugated polymers (that we will refer to as the conjugation breaking model) considers the polymer as a set of segments along which the wave function is delocalized. The region of extension of the wave function is limited by the break of conjugation which occurs when the torsion angle between the two neighboring rings in the chain is sufficiently large.[14−17] In such a picture, the long wave functions have energies close to the band edge, while due to quantum confinement effects short wave functions have energies further away from the band edge. This implies that near band edge states are less localized than the ones further away from the band edge. This picture also implies a fixed band edge energy equal to the one of an infinite polymer chain. On the other hand, it is known that in one-dimensional disordered systems the electronic states are localized, with the localization length that is smallest close to the band edge.[18] It is not unreasonable to expect that disordered conjugated polymers might fall within

Received: December 2, 2010
Revised: December 30, 2010
Published: February 3, 2011

such class of systems, which would imply that the near band-edge states are the most localized.

In this work, we focus on a widely used and studied poly(3-hexylthiophene) (P3HT) polymer and the density and wave function localization of hole states. Our calculations give answers to the open questions mentioned above about the functional form of the density of states and the dependence of localization properties on energy of states near the band edge. Furthermore, we provide insight into the origin of the band edge state localization and identify a simple model that captures the essential features of the electronic structure of the system.

THEORY

From the theoretical point of view, the problem of understanding the density of electronic states and wave function localization properties is quite challenging. The main reason for that is the large statistics necessary to get sufficient information about the electronic states in the spectral region close to the band edge. In past years, the construction of the atomic structure of disordered polymer systems using classical molecular dynamics simulations has become a regular practice.[16,17,19−25] However, the main issue remains how to calculate the electronic structure of such systems. The calculations within density functional theory (DFT) are typically limited to around a thousand atoms and can be quite computationally expensive. The calculation on the system of that size yields however only a few (say 5−10) states in the spectral region of interest for transport properties (say within 0.5 eV from the band edge). This certainly does not give sufficient statistics to get information about the density of states and wave function localization.

Consequently, there is a great need for faster but still sufficiently accurate methodologies for the calculation of electronic structure of polymers. In our recent works, we have developed a fast method for the construction of single particle Kohn−Sham Hamiltonian that has the accuracy similar as DFT, the charge patching method (CPM),[23,26] as well as a very efficient method for the diagonalization of the constructed Hamiltonian, the overlapping fragments method (OFM).[27]

The CPM is based on the idea that the contribution of a given atom to the electronic charge density of the system (so-called charge density motif) depends mainly on its local bonding environment. The total electronic charge density of the system is then constructed by adding the charge density motifs of all atoms in the system. The motifs are extracted from DFT calculations on a small prototype system where atoms have the same bonding environment as in the large system of interest. With charge density at hand, one can then easily construct the single particle Kohn−Sham Hamiltonian by solving the Poisson equation for the Hartree potential and using the local density approximation (LDA) formula for the exchange correlation potential.

In the OFM, the Hamiltonian constructed from CPM is represented in the basis of eigenstates of small fragments that the system is divided into. The choice of fragments is based on physical intuition from following considerations. The P3HT polymer consists of the main thiophene chain where electronic states in the spectral region near the band gap are localized and side alkyl chains which are not very relevant for electronic properties. Therefore, each of the fragments consists of small oligomers of the main thiophene chain. We found that the simple partitioning of the polymer into mutually nonoverlapping oligomers would not give a sufficiently good basis set, since it does not represent well the wave function in the region of the bond that connects the monomers. Therefore, the fragment oligomers have to be mutually overlapping. To accurately describe the electronic structure in the certain spectral region (say within 0.5 eV) near the band edge, one needs just a few eigenstates of the fragment oligomer regardless of the size of the whole system. With basis wave functions at hand, one then further evaluates the transfer and overlap integrals between wave function of each fragment and the fragments in its neighborhood (in the same chain and in the other chains) and solves the generalized eigenvalue problem. Since the size of the basis set scales linearly with the size of the system, the whole evaluation of basis wave functions and transfer and overlap integrals scales linearly as well. Furthermore, the evaluations of the wave functions of different fragments can be performed in parallel on different groups of processors. The same is the case for the evaluation of transfer and overlap integrals, which makes the whole methodology well-suited for making good use of parallel computing architectures.

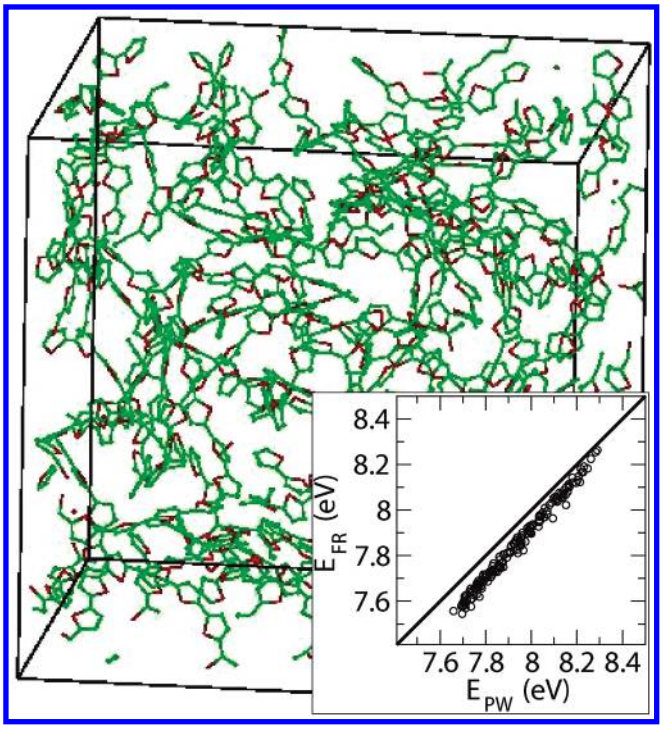

Figure 1. Atomic structure of one of the realizations of the system consisting of 12 P3HT chains, each one being 40 units long (12024 atom system). Alkyl side chains have been removed for clarity but are fully taken into account in the calculation. The inset shows the comparison of eigenenergies obtained by the diagonalization in the basis of fragment HOMOs (E_{FR}) and the plane wave basis (E_{PW}) for 10 different 2510 atom systems.

We generate the atomic structure from classical molecular dynamics using a simulated annealing procedure, as it is widely done in the literature[16,19,20,24,25] and as has been done in our previous works.[23] To calculate the density of states of the amorphous P3HT polymer we generate 50 different realizations (one of these is shown in Figure 1) of the atomic structure of the system consisting of 12 chains, each one being 40 units long. Each unit of the polymer consists of a thiophene molecule with a hexyl side chain and contains 25 atoms (26 atoms in the case of a unit at the end of the chain), and therefore the whole system

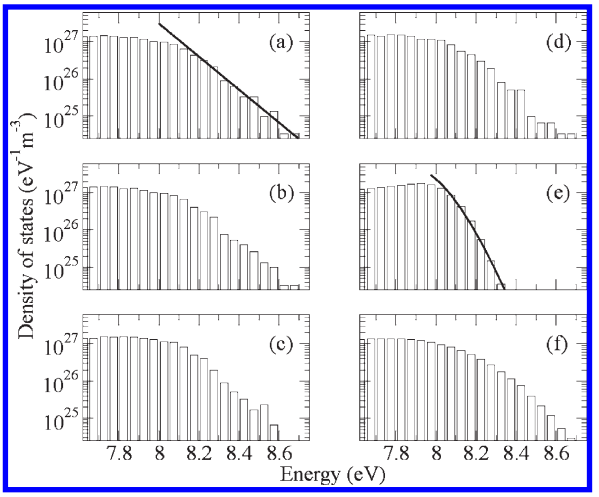

Figure 2. Density of states of disordered P3HT polymer: (a) full calculation; (b) in the absence of interchain electronic coupling; (c) in the presence of electronic coupling with nearest neighbors only ; (d) in the presence of electronic coupling with nearest neighbors only, with constant overlap $t = 0.85$ eV; (e) in a model with uncorrelated on-site t_{mm} elements with Gaussian distribution ($\sigma = 0.256$ eV and $\mu = 6.24$ eV) and electronic coupling with nearest neighbors only with $t = 0.85$ eV; (f) same as e, but with correlated on-site elements whose correlation function was extracted from the calculations of t_{mm} elements.

contains 12 024 atoms. The charge density and the single particle Hamiltonian of each of these are then constructed using the CPM and the eigenstates obtained using the OFM. The accuracy of the CPM for the system at hand was tested by a comparison with direct DFT/LDA calculation for a smaller 756 atom system, where it is still feasible to do a DFT calculation. We compare the density of states obtained by the two methods, as well as the on-site Hamiltonian matrix elements (to be defined later in the text). The latter are the most important parameters for the electronic structure of the system, as will be shown in this work. The results, presented in Supporting Information, indicate an excellent agreement between DFT/LDA and CPM calculation. In the OFM, we choose the basis consisting of a single HOMO from each thiophene trimer fragment with propyl side chains.[27] We have checked that such a basis gives a good accuracy, as can be seen from the inset in Figure 1, where the results are compared with the ones obtained directly in the plane wave basis, in the case of 10 different 2510 atom systems. Furthermore, such a simple basis facilitates the interpretation of the results.

RESULTS AND DISCUSSION

The density of states obtained from our calculations is presented in Figure 2a. We find that the density of states in the region from 8.2 to 8.7 eV can be fitted very well with an exponential distribution $D(E) = D_0 \exp[-(E - E_0)/E_b]$, with $E_0 = 8.2$ eV, $E_b = 98$ meV, and $D_0 = 3.98 \times 10^{26}$ eV^{-1}m^{-3} (the fit is shown in Figure 2a). We test the hypothesis that the obtained data have the mentioned distribution using the χ^2-test.[28] We obtain the $X^2 = \sum_{i=1}^{n}(O_i - F_i)^2/F_i$ (where $n = 10$ is the number of intervals in the 8.2−8.7 eV range, while O_i and F_i are the number of observed and expected eigenstates in interval i) value of 4.91, which implies an 84% confidence of the validity of the hypothesis. On the other hand, if we try to fit our data in the same spectral region with a Gaussian distribution $D(E) = D_0 \exp[-(E - E_0)^2/E_b^2]$, where E_0 takes reasonable values near 8.2 eV (in the interval from 8 to 8.4 eV), the smallest X^2 that we get is 13, which implies the confidence of 16% or less.

We next discuss the value of the exponential density of states width parameter E_b in terms of the fits of the density of states to the experimental polythiophene field-effect transistor mobility measurements available in the literature. In ref 29, a fit to the Vissenberg−Matters model[6] that contains the exponential density of states gives the E_b value in the 27−32 meV range depending on the processing conditions. The fit to the mobility edge model, which also assumes the exponential density of states in the tail, but a different distribution away from the tail, gives E_b in the range from 30 to 60 meV. One should note that the measurements in ref 29 are performed for ordered, high-mobility polymers (which can be witnessed for example by low activation energies of the order of 50 meV, much smaller than activation energies in fully disordered P3HT which can reach 350 meV[30−32]). Therefore it is quite expected that the E_b obtained from our simulation of fully disordered polymer is larger than E_b obtained in ref 29. The role of disorder on the E_b parameter was also nicely experimentally illustrated in ref 29 where processing conditions which lead to a more ordered structure gave smaller values of E_b. Other experimental results on P3HT give E_b values that span a similar range: 59 meV (ref 33), 37 meV (ref 30), and 40−65 meV (ref 34). One should however keep in mind that the density of states parameters extracted from fits of the mobility to models should always be taken with caution, due to the uncertainty of the correctness of the underlying assumptions of the models.

To understand the wave function localization properties, we calculate the localization length for each of the calculated states. For a wave function represented in a localized and orthonormal basis $|\Psi\rangle = \sum_m d_m|m\rangle$, the localization length can be defined as $L = 1/\sum_m |d_m|^4$. The basis of HOMOs of trimers $|i\rangle$ is not orthonormal, so we first orthonormalize it by making a transformation[35] $|m\rangle = \sum_i T_{mi}|i\rangle$, with $T = (S^{-1/2})^*$, where S is the overlap matrix whose elements are given as $S_{ij} = \langle i|j\rangle$. The orthonormalized wave functions $|m\rangle$ have a similar degree of localization as the original wave functions $|i\rangle$. The wave function expansion coefficients in the orthonormal basis $|m\rangle$ are then related to the coefficients c_i in the basis i via $d_m = \sum_i (S^{1/2})_{mi} c_i$. The dependence of the localization length on the energy of the electronic state is shown in Figure 3a. The states near the band edge are well-localized (to ∼5 monomers), while as one moves away from it the states that are more extended start to appear. However, we do not find any mobility edge in the sense that, below that edge, all of the states become extended.

We would like further to understand the factors that determine the observed density of states and localization lengths. On this route, one has first to understand what is the dimensionality of the system considered. While the system is inevitably located in three-dimensional space, there is a possibility that it can be simply considered as a superposition of one-dimensional polymer chains. To test if this is the case, we turn off the interchain electronic coupling, by setting to zero all of the Hamiltonian matrix elements $t_{mn} = \langle m|H|n\rangle$, where m and n belong to different chains. The density of states obtained that way is shown in Figure 2b. A comparison with the density of states in the presence of interchain electronic coupling (Figure 2a) suggests that interchain electronic coupling does not have any significant effect on the density of states. Furthermore, the plot of the wave functions in the two cases (Figure 4b,c) indicates that practically all wave functions remain unchanged by the presence/absence of

dx.doi.org/10.1021/jp1114527 |J. Phys. Chem. B 2011, 115, 1792–1797

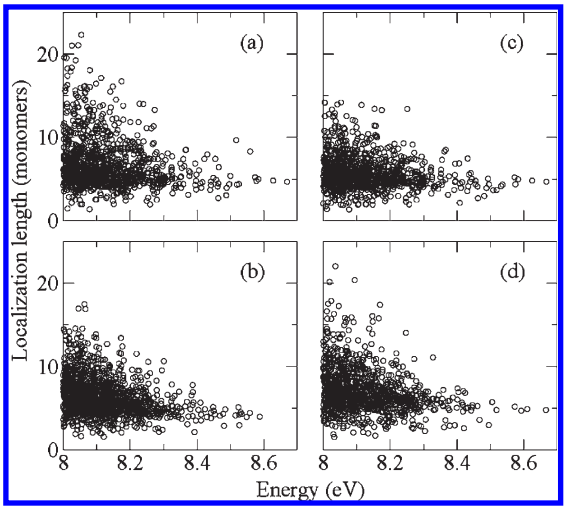

Figure 3. Dependence of localization length on energy of the top hole states in disordered P3HT polymer: (a) the results obtained without any additional assumptions; (b) in the absence of interchain electronic coupling; (c) in the presence of electronic coupling with nearest neighbors only; (d) in the presence of electronic coupling with nearest neighbors only and with a constant nearest neighbors overlap $t = 0.85$ eV.

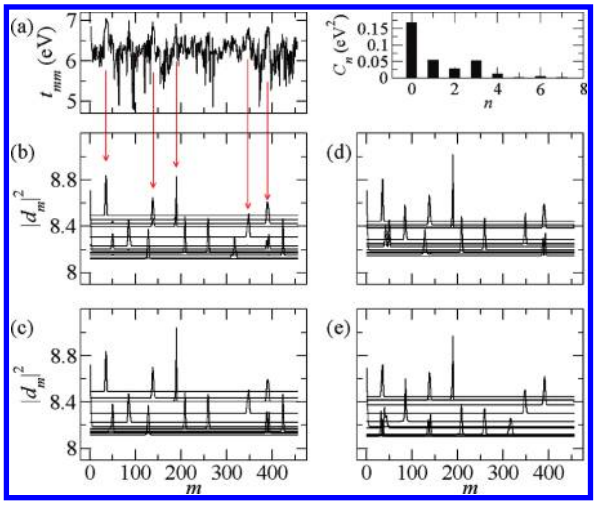

Figure 4. On-site Hamiltonian matrix elements t_{mm} (m is the index of the site on the chain) and the top hole wave functions for one realization of a disordered P3HT polymer system: (a) the on-site Hamiltonian matrix elements and their correlation function defined as $C_n = \langle (t_{mm} - \langle t \rangle)(t_{m+n,m+n} - \langle t \rangle) \rangle$; (b) the wave functions (each curve is one wave function); (c) the wave functions in the system with no interchain coupling; (d) the wave functions in the presence of electronic coupling with nearest neighbors only; (e) the wave functions in the presence of electronic coupling with nearest neighbors only and with a constant nearest neighbor overlap t = 0.85 eV.

interchain electronic coupling and that most of the wave functions are localized in one chain. Only occasionally the two wave functions from different chains can get hybridized by interchain electronic coupling, such as wave functions of HOMO-1 and HOMO-3 in Figure 4b. As a consequence, the dependence of the localization length on energy is similar in both cases and reaches slightly larger values in the case with interchain coupling (see Figure 3a,b), due to mentioned hybridization effects. This discussion nevertheless shows that, for all practical purposes, interchain electronic coupling is negligible for disordered P3HT. As a consequence, to understand the density of states and wave function localization properties of the whole system, it is sufficient to understand these properties for individual polymer chains. One should still keep in mind that the Hamiltonian matrix elements between the orthonormal basis states of the same chain still depend on the presence of other chains that introduce the long-range electrostatic potential. Our conclusions about the role of interchain coupling refer to amorphous P3HT polymers. In crystalline form of P3HT, where high values of mobility were obtained,[36,37] there is a significant interchain coupling that causes the delocalization of carriers in two dimensions.

To understand the factors that determine the wave function localization, in Figure 4a,b, we plot the on-site Hamiltonian matrix elements t_{mm} and the wave functions of top hole states. One easily recognizes from the figure, as emphasized by arrows, that top hole states are located in the regions of highest local maxima of on-site matrix elements. The fluctuations in t_{mm} originate from the fluctuations of electrostatic potential along the chain (Figure 2 in Supporting Information indicates that the CPM reproduces these on-site fluctuations accurately when compared with direct DFT/LDA calculations). Therefore, Figure 4a,b suggests that the disorder in electrostatic potential localizes the wave functions. Such a picture is quite different than the usual conjugation breaking picture, where the wave function is localized in the region between the two conjugation breaks, caused by large values of torsion angles between neighboring rings and manifested in small values of nearest neighbor off-site elements $t_{m,m+1}$ at the breaking point. In the conjugation breaking picture, the off-site elements therefore determine the localization region. To reliably identify the influence of off-site elements on localization properties, we make further simplifications to the Hamiltonian.

We first restrict the Hamiltonian matrix to include only the on-site and off-site nearest neighbor matrix elements, which gives it a form of a nearest neighbor tight-binding model. This is a good approximation as can be evidenced by comparison of Figure 4c and d and Figure 2b and c, as well as Figure 3b and c, which all indicate that properties of interest do not change significantly. The distribution of on-site and nearest neighbor off-site matrix elements is shown in Figure 5. To understand the role of nearest neighbor off-site elements on localization properties, we make a drastic simplification by setting all of them to a constant value of $t = 0.85$ eV, which is the most probable value of the distribution shown in Figure 5 (top part). After such a drastic change, the wave functions still remain in the same position (Figure 4e), and the density of states of the system is still very similar as before (Figure 2d). This clearly indicates that the role of off-site elements on the localization properties and the density of states is only minor. Consequently, one can certainly not think of the localization process in terms of the conjugation breaking model.

In past few years, there have been several works where the adequacy of conjugation breaking picture for the description of excitons in conjugated polymers was discussed. In polymers with high barrier for interring torsions (such as PPV), conjugation breaking in the classical sense does not occur, and such polymers were modeled by the Anderson model with weak disorder.[38,39] In these polymers, the presence of weak conformational disorder leads to Anderson localization. On the other hand, polymers with low barrier for interring torsions (such as P3HT) contain the conjugation breaks. It was however shown in ref 40 that the conjugation breaks do not necessarily localize the excitons; their

dx.doi.org/10.1021/jp1114527 |J. Phys. Chem. B 2011, 115, 1792–1797

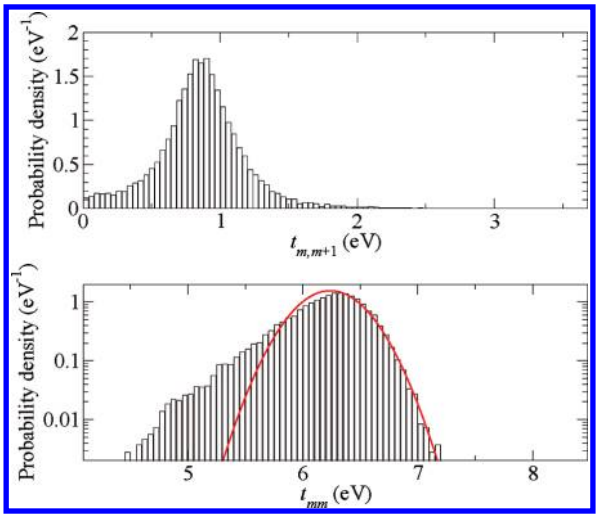

Figure 5. Histogram of appearance of nearest neighbor off-site Hamiltonian matrix elements (top) and on-site Hamiltonian matrix elements (bottom). The curve represents a fit of the latter to the Gaussian distribution.

localization is determined by the interplay of the conformational disorder (beyond the effect of conjugation breaking) and conjugation breaking. In particular, it has been proposed[40] that conjugation breaks induce the localization only in the case when localization length introduced by conformational disorder is comparable to the distance between two conjugation breaks. Although these results concern the excitons, rather than our case of charge carriers, these seem to be consistent with our conclusion that the conjugation break model is an oversimplified picture of the localization process. The conjugation breaking picture for excitons was also questioned in ref 41. On the basis of the calculation of a straight polymer chain with a single torsion defect, the authors concluded that conjugation breaking does not localize the exciton. Such a conclusion is in slight discrepancy with ref 40 due to the fact that such a calculation does not include the conformational disorder beyond the conjugation breaking effect. On the experimental side, there are suggestions[42] that P3HT cannot be modeled as a set of coupled chromophores induced by conjugation breaks. On the other hand, such models were successful in explaining the ultrafast exciton relaxation in PPV[43] but still suggest that the disorder in chromophore energies caused by conformational disorder, plays a deciding role in exciton localization.

We would like to further understand what is the minimal information required about the on-site Hamiltonian matrix elements to reliably reproduce the tail of the density of states and therefore identify the main parameters that determine the density of states. The upper tail of the distribution of on-site matrix elements shown in Figure 5 (bottom part) can be excellently replaced with a Gaussian distribution $g(E) = (1/\sigma(2\pi)^{1/2})\exp[-(E-\mu)^2/2\sigma^2]$ with parameters $\sigma = 0.256$ eV and $\mu = 6.24$ eV. It has been established in the literature[18] that the nearest neighbor tight-binding model with Gaussian distribution of on-site energies and constant off-site matrix element t gives the density of states in the tail of the form $\sim\exp[-\alpha(E-E_v)^{3/2}]$, where $E_v = \mu + 2t$ is the valence band edge in the absence of disorder. Our numerical results for the density of states of such model are shown in Figure 2e. The tail agrees with the expected $\sim\exp[-\alpha(E-E_v)^{3/2}]$ form (the curve that represents the fit of the tail to this form is also shown in Figure 2e) and differs from the previously obtained density of states. This difference suggests that more information than simple distribution of on-site elements is required for the description of the density of states. The additional missing information is the correlations between on-site energies. We therefore calculate for each n the correlation function between on-site elements of sites m and $m + n$. We then generate the on-site elements with Gaussian distribution and with correlation function equal to the calculated one. The density of states obtained from such a model is shown in Figure 2f. It greatly improves over the one in Figure 2e and largely matches the previous ones. Consequently, one can conclude that the density of states of disordered P3HT can be largely understood from the model with correlated Gaussian distributed on-site energies and constant off-site couplings.

CONCLUSION

Using the latest developments in the methodology for the calculation of electronic structure of organic systems, we have been able for the first time to generate sufficient statistics to extract the tail of the density of electronic states in a disordered polymer material and found that it can be described by an exponential distribution. The analysis of the results yielded important conclusions about the factors that determine the localization of the hole states in the tail of the density of states. Their positions and localization length are mainly determined by the disordered electrostatic potential. Therefore, the electronic structure of the system cannot be described by conventional tight-binding models parametrized from single straight chain calculations, as they miss the long-range electrostatic potential. We have consequently proposed a tight-binding model that incorporates the disordered electrostatic potential through random values of on-site energies, that exhibit a Gaussian distribution with correlations among several neighboring sites. While our calculation was focused on hole states, which are of most interest for organic semiconductors, we expect qualitatively the same behavior for electron states.

ASSOCIATED CONTENT

Supporting Information. The comparison of DFT and CPM calculations. This material is available free of charge via the Internet at http://pubs.acs.org.

AUTHOR INFORMATION

Corresponding Author
*E-mail: nenad.vukmirovic@ipb.ac.rs.

ACKNOWLEDGMENT

This work was supported by the DMS/BES/SC of the U.S. Department of Energy under Contract No. DE-AC02-05CH11231. It used the resources of National Energy Research Scientific Computing Center (NERSC) and the INCITE project allocations within the National Center for Computational Sciences (NCCS). In the last stages of this work, N.V. was supported by the Ministry of Science and Technological Development of the Republic of Serbia, under project No. ON171017, and the European Commission under EU FP7 projects PRACE-1IP, HP-SEE, and EGI-InSPIRE.

REFERENCES

(1) Li, G.; Shrotriya, V.; Huang, J. S.; Yao, Y.; Moriarty, T.; Emery, K.; Yang, Y. *Nat. Mater.* **2005**, *4*, 864–868.
(2) Dodabalapur, A.; Torsi, L.; Katz, H. E. *Science* **1995**, *268*, 270–271.
(3) Friend, R. H.; Gymer, R. W.; Holmes, A. B.; Burroughes, J. H.; Marks, R. N.; Taliani, C.; Bradley, D. D. C.; Santos, D. A. D.; Brédas, J. L.; Lögdlund, M.; Salaneck, W. R. *Nature (London)* **1999**, *397*, 121–128.
(4) Colvin, V. L.; Schlamp, M. C.; Alivisatos, A. P. *Nature (London)* **1994**, *370*, 354–357.
(5) Arkhipov, V. I.; Heremans, P.; Emelianova, E. V.; Adriaenssens, G. J.; Bassler, H. *Appl. Phys. Lett.* **2003**, *82*, 3245–3247.
(6) Vissenberg, M. C. J. M.; Matters, M. *Phys. Rev. B* **1998**, *57*, 12964–12967.
(7) Pasveer, W. F.; Cottaar, J.; Tanase, C.; Coehoorn, R.; Bobbert, P. A.; Blom, P. W. M.; de Leeuw, D. M.; Michels, M. A. J. *Phys. Rev. Lett.* **2005**, *94*, 206601.
(8) Borsenberger, P. M.; Pautmeier, L.; Bassler, H. *J. Chem. Phys.* **1991**, *94*, 5447–5454.
(9) Baranovskii, S. D.; Cordes, H.; Hensel, F.; Leising, G. *Phys. Rev. B* **2000**, *62*, 7934–7938.
(10) Arkhipov, V. I.; Emelianova, E. V.; Adriaenssens, G. J. *Phys. Rev. B* **2001**, *64*, 125125.
(11) Vukmirović, N.; Wang, L.-W. *Appl. Phys. Lett.* **2010**, *97*, 043305.
(12) Tal, O.; Rosenwaks, Y.; Preezant, Y.; Tessler, N.; Chan, C. K.; Kahn, A. *Phys. Rev. Lett.* **2005**, *95*, 256405.
(13) Hulea, I. N.; Brom, H. B.; Houtepen, A. J.; Vanmaekelbergh, D.; Kelly, J. J.; Meulenkamp, E. A. *Phys. Rev. Lett.* **2004**, *93*, 166601.
(14) Kohler, B. E.; Woehl, J. C. *J. Chem. Phys.* **1995**, *103*, 6253–6256.
(15) Yaliraki, S. N.; Silbey, R. J. *J. Chem. Phys.* **1995**, *104*, 1245–1253.
(16) Yang, H.-C.; Hua, C.-Y.; Kuo, M.-Y.; Huang, Q.; Chen, C.-L. *ChemPhysChem* **2004**, *5*, 373–381.
(17) Ruhle, V.; Kirkpatrick, J.; Andrienko, D. *J. Chem. Phys.* **2010**, *132*, 134103.
(18) Kramer, B.; MacKinnon, A. *Rep. Prog. Phys.* **1993**, *56*, 1469–1564.
(19) Kilina, S.; Batista, E.; Yang, P.; Tretiak, S.; Saxena, A.; Martin, R. L.; Smith, D. *ACS Nano* **2008**, *2*, 1381–1388.
(20) Yang, P.; Batista, E. R.; Tretiak, S.; Saxena, A.; Martin, R. L.; Smith, D. L. *Phys. Rev. B* **2007**, *76*, 241201.
(21) McMahon, D. P.; Troisi, A. *Chem. Phys. Lett.* **2009**, *480*, 210–214.
(22) Cheung, D. L.; McMahon, D. P.; Troisi, A. *J. Am. Chem. Soc.* **2009**, *131*, 11179–11186.
(23) Vukmirović, N.; Wang, L.-W. *J. Phys. Chem. B* **2009**, *113*, 409–415.
(24) Zhang, G.; Pei, Y.; Ma, J.; Yin, K.; Chen, C.-L. *J. Phys. Chem. B* **2004**, *108*, 6988–6995.
(25) Zhang, G.; Ma, J.; Wen, J. *J. Phys. Chem. B* **2007**, *111*, 11670–11679.
(26) Vukmirović, N.; Wang, L.-W. *J. Chem. Phys.* **2008**, *128*, 121102.
(27) Vukmirović, N.; Wang, L.-W. http://arxiv.org; citation 1011.4764v1 (accessed February 1, 2011).
(28) Plackett, R. L. *Int. Stat. Rev.* **1983**, *51*, 59–72.
(29) Salleo, A.; Chen, T. W.; Völkel, A. R.; Wu, Y.; Liu, P.; Ong, B. S.; Street, R. A. *Phys. Rev. B* **2004**, *70*, 115311.
(30) Tanase, C.; Meijer, E. J.; Blom, P. W. M.; de Leeuw, D. M. *Phys. Rev. Lett.* **2003**, *91*, 216601.
(31) Craciun, N. I.; Wildeman, J.; Blom, P. W. M. *Phys. Rev. Lett.* **2008**, *100*, 056601.
(32) Vukmirović, N.; Wang, L.-W. *Nano Lett.* **2009**, *9*, 3996–4000.
(33) Nolasco, J. C.; Cabre, R.; Ferre-Borrull, J.; Marsal, L. F.; Estrada, M.; Pallares, J. *J. Appl. Phys.* **2010**, *107*, 044505.
(34) Gburek, B.; Wagner, V. *Org. Electron.* **2010**, *11*, 814–819.
(35) Lowdin, P.-O. *J. Chem. Phys.* **1950**, *18*, 365–375.
(36) Sirringhaus, H.; Brown, P. J.; Friend, R. H.; Nielsen, M. M.; Bechgaard, K.; Langeveld-Voss, B. M. W.; Spiering, A. J. H.; Janssen, R. A. J.; Meijer, E. W.; Herwig, P.; de Leeuw, D. M. *Nature (London)* **1999**, *401*, 685–688.
(37) Dicker, G.; Savenije, T. J.; Huisman, B.-H.; Leeuw, D. M. D.; de Haas, M. P.; Warman, J. M. *Synth. Met.* **2003**, *137*, 863–864.
(38) Barford, W.; Trembath, D. *Phys. Rev. B* **2009**, *80*, 165418.
(39) Makhov, D. V.; Barford, W. *Phys. Rev. B* **2010**, *81*, 165201.
(40) Barford, W.; Lidzey, D. G.; Makhov, D. V.; Meijer, A. J. H. *J. Chem. Phys.* **2010**, *133*, 044504.
(41) Beenken, W. J. D.; Pullerits, T. *J. Phys. Chem. B* **2004**, *108*, 6164–6169.
(42) Wells, N. P.; Blank, D. A. *Phys. Rev. Lett.* **2008**, *100*, 086403.
(43) Dykstra, T. E.; Hennebicq, E.; Beljonne, D.; Gierschner, J.; Claudio, G.; Bittner, E. R.; Knoester, J.; Scholes, G. D. *J. Phys. Chem. B* **2009**, *113*, 656–667.